

Observation of lower to higher bandgap transition of one-dimensional defect modes

Xiaosheng Wang*, Jack Young, and Zhigang Chen

Department of Physics and Astronomy, San Francisco State University, CA 94132

and TEDA Applied Physics School, Nankai University, Tianjin, China

* Visiting from Sun Yat-sen Univ., Guangzhou, China

zchen@stars.sfsu.edu

Doug Weinstein and Jianke Yang

Department of Mathematics and Statistics, University of Vermont, VT 05401

and Zhou Pei-Yuan Center for Applied Mathematics, Tsinghua Univ., Beijing, China.

Abstract: We demonstrate one-dimensional optically-induced photonic lattices with a negative defect and observe linear bandgap guidance in such a defect. We show that a defect mode moves from the first bandgap to a higher bandgap as the lattice potential is increased. Our experimental results are in good agreement with the theoretical analysis of these effects.

© 2006 Optical Society of America

OCIS codes: (999.9999) Photonic bandgaps; (190.0190) Nonlinear optics; (230.4000) Microstructure.

References and links

1. J. D. Joannopoulos, R. D. Meade, and J. N. Winn, *Photonic Crystals: Molding the Flow of Light* (Princeton, NJ, 1995).
2. P. Russell, "Photonic crystal fibers," *Science* **299**, 358 (2003).
3. S. L. McCall, P. M. Platzman, R. Dalichaouch, D. Smith, and S. Schultz, "Microwave propagation in two-dimensional dielectric lattices," *Phys. Rev. Lett.* **67**, 2017 (1991).
4. F. Luan, A. K. George, T. D. Hedley, G. J. Pearce, D. M. Bird, J. C. Knight, and P. St. J. Russell, "All-solid photonic bandgap fiber," *Opt. Lett.* **29**, 2369 (2004).
5. A. Argyros, T. A. Birks, S. G. Leon-Saval, C. B. Cordeiro, F. Luan, and P. St. J. Russell, "Photonic bandgap with an index step of one percent," *Opt. Express* **13**, 309 (2005).
6. J. Schmidtke, W. Stille, and H. Finkelmann, "Defect Mode Emission of a Dye Doped Cholesteric Polymer Network", *Phys. Rev. Lett.* **90**, 083902 (2003).
7. X. Wu, A. Yamilov, X. Liu, S. Li, V. P. Dravid, R. P. H. Chang, and H. Cao, "Ultraviolet photonic crystal laser," *Appl. Phys. Lett.* **85**, 3657 (2004).
8. D. Mandelik, H. S. Eisenberg, Y. Silberberg, R. Morandotti, and J. S. Aitchison, "Band structure of waveguide arrays and excitation of Floquet-Bloch solitons," *Phys. Rev. Lett.* **90**, 53902 (2003).
9. N. K. Efremidis, J. Hudock, D. N. Christodoulides, J. W. Fleischer, O. Cohen, and M. Segev, "Two-Dimensional optical lattice solitons," *Phys. Rev. Lett.* **91**, 213906 (2003).
10. A. A. Sukhorukov, D. Neshev, W. Krolikowski, and Y. S. Kivshar, "Nonlinear Bloch-wave interaction and Bragg scattering in optically induced lattices," *Phys. Rev. Lett.* **92**, 093901 (2004).
11. U. Peschel, R. Morandotti, J. S. Aitchison, H. S. Eisenberg, and Y. Silberberg, "Nonlinearly induced escape from a defect state in waveguide arrays," *Appl. Phys. Lett.* **75**, 1348 (1999).
12. R. Morandotti, H. S. Eisenberg, D. Mandelik, Y. Silberberg, D. Modotto, M. Sorel, C. R. Stanley, and J. S. Aitchison, "Interactions of discrete solitons with structural defects," *Opt. Lett.* **28**, 834 (2003).
13. F. Fedele, J. Yang, and Z. Chen, "Defect modes in 1D photonic lattices," *Opt. Lett.* **30**, 1506 (2005).
14. F. Fedele, J. Yang, and Z. Chen, "Properties of defect modes in one-dimensional optically-induced photonic lattices," *Stud. Appl. Math.*, **115** 279 (2005).
15. D. Christodoulides and R. Joseph, "Discrete self-focusing in nonlinear arrays of coupled waveguides," *Opt. Lett.* **13**, 794 (1988).
16. J. W. Fleischer, M. Segev, N. K. Efremidis, and D. N. Christodoulides, "Observation of two-dimensional discrete solitons in optically induced nonlinear photonic lattices," *Nature (London)* **422**, 147 (2003).
17. D. Neshev, E. Ostrovskaya, Y. Kivshar, and W. Krolikowski, "Spatial solitons in optically induced gratings," *Opt. Lett.* **28**, 710 (2003).

18. H. Martin, E.D. Eugenieva, Z. Chen, and D.N. Christodoulides, "Discrete solitons and soliton-induced dislocations in partially-coherent photonic lattices," *Phys. Rev. Lett.* **92**, 123902 (2004).
 19. Z. Chen and K. McCarthy, "Spatial soliton pixels from partially coherent light," *Opt. Lett.* **27**, 2019 (2002).
 20. X. Wang, Z. Chen, and J. Yang, "Guiding light in optically-induced ring lattices with a low refractive index core", *Opt. Lett.* **31**, 1887 (2006).
 21. I. Makasyuk, Z. Chen, and J. Yang, "Band-Gap Guidance in Optically Induced Photonic Lattices with a Negative Defect", *Phys. Rev. Lett.*, **96**, 223903 (2006).
 22. P. Yeh, and A. Yariv, "Bragg reflection waveguides", *Opt. Commun.* **19**,427 (1976).
 23. Y. Cho, A. Yariv, and P. Yeh, "Observation of confined propagation in Bragg waveguides", *Appl. Phys. Lett.* **30**, 471 (1977).
 24. H. Trompeter, U. Peschel, T. Pertsch, F. Lederer, U. Streppel, D. Michaelis, and A. Bräuer, "Tailoring guided modes in waveguide arrays", *Opt. Exp.* **11**, 3404 (2003).
 25. L. Morales-Molina and R. A. Vicencio, "Trapping of discrete solitons by defects in nonlinear waveguide arrays", *Opt. Lett.*, **31**, 966 (2006).
 26. M. J. Ablowitz, B. Ilan, E. Schonbrun, and R. Piestun, "Solitons in two-dimensional lattices possessing defects, dislocations and quasicrystal structures. *Phys. Rev. E*, preprint.
-

It is well known that one of the unique and most interesting features of the photonic band-gap (PBG) structures is a fundamentally different way of waveguiding by defects in otherwise uniformly periodic structures as opposed to conventional guidance by total internal reflection. Such a waveguiding property has been demonstrated with an "air-hole" in photonic crystal fibers (PCF) for optical waves [1, 2], in an isolated defect in two-dimensional arrays of dielectric cylinders for microwaves [3], and recently in all-solid PCF with a lower-index core [4, 5]. In fact, PBG guidance has been studied for a wide range of spectra, and laser emission based on photonic defect modes (DMs) has been realized in a number of experiments [6, 7].

In photonic crystals and PCF, bandgap guidance is associated with the time-domain frequency modes where the propagation constant is imaginary (i.e., propagation forbidden – band gaps). Within the gaps, frequency modes cannot exist but light can be localized by defects that support evanescent defect states [1-5]. On the other hand, the analyses of how a monochromatic light field distributes in waveguide lattices often focus on the bandgaps of spatial frequency modes (i.e., propagation constant vs. transverse wave vector) [8-10]. In one-dimensional (1D) fabricated waveguide arrays, previous experiments have investigated nonlinearly induced escape from a defect state [11] and interactions of discrete solitons with structural defects [12]. In optically-induced photonic lattices such as those created in photorefractive crystals, recent work has also revealed the existence of linear DMs [13, 14]. Although nonlinear discrete solitons in uniform lattices without defects have been observed in a number of experiments [15-18], demonstration of PBG guidance at different bandgaps of the lattices with defects has remained a challenge.

In this paper, we report the demonstration of light confinement as DMs in optically-induced 1D photonic lattices with a single-site negative defect. In such a defect, the lattice intensity is lower than that at nearby sites (akin to an "air defect" in photonic crystals [1, 2]), so light has a tendency to escape from the defect site rather than to be confined in it. However, as predicted recently [13], localized DMs do exist under appropriate conditions due to repeated Bragg reflections. Experimentally, we first create a single-site negative defect by optical induction, which maintains its identity as a defect through a 20-mm-long photorefractive crystal. We then launch a quasi-1D Gaussian probe beam into the defect and observe the formation of localized DMs. Such light localization does not come from the nonlinear self-action of the probe beam itself, nor does it come from the traditional total-internal-reflection guidance. Furthermore, we demonstrate a DM transition from a lower bandgap (between first and second Bloch bands) to a higher bandgap (between second and third Bloch bands) by fine-tuning the lattice potential.

Our experimental setup shown in Fig. 1 is similar to those used in our previous work [18, 19], but here we focus on 1D lattices with a defect. The defect is created by launching into a SBN crystal a partially incoherent light beam ($\lambda=488$ nm) spatially modulated by a specially-designed amplitude mask, which gives rise to a periodic input intensity pattern with a defect as shown in Fig. 2(a). This intensity pattern remains nearly unchanged through the 20-mm long crystal under appropriate conditions [Fig. 2(b)], as achieved by suppressing the Talbot effect with spatial filtering and employing a weak nonlinearity. By fine-tuning the nonlinearity (or the index change) as controlled by the lattice beam intensity, polarization, and the bias field [16-19], the lattice structure with the defect remains throughout the crystal. For probing the defect, a cylindrically-focused laser beam of FWHM $16\ \mu\text{m}$ [Fig. 2(c)] is aimed into the defect site, propagating collinearly with the lattice beam. The probe is extraordinarily polarized, but it is either very weak (for $\lambda=488$ nm, as in Fig. 2) or at a photorefractive insensitive wavelength ($\lambda=632.8$ nm, as in Fig. 3 and Fig. 5 below) so it does not experience any nonlinear self-action. Typical results of bandgap guidance are shown in Fig. 2(d), where good confinement of the probe beam by the defect channel is obtained. Such guidance is not attributed to total internal reflection because the defect forms an anti-guide in the self-focusing crystal. When the lattice beam is removed, the probe beam alone does not exhibit self-focusing under the same bias field.

One of the interesting characteristics of linear DMs is that, like discrete solitons, they can only exist in certain parameter regions, and they typically have “tails” if less localized. Since a DM bifurcates from the edge of a Bloch band, its “tails” have different symmetry and phase distributions in order to “match” the Bloch waves in a given band [13]. Under proper lattice conditions, a Gaussian probe beam can evolve into a *symmetric* DM which has part of its energy concentrated in the defect site while the tails have characteristic intensity and phase profiles. By examining those features and comparing with the theory, one can determine in which bandgap the DM is located. Experimentally, we have demonstrated a controlled transition of DMs from a lower bandgap [between first and second bands] to a higher bandgap [between second and third bands] by fine-tuning the bias field.

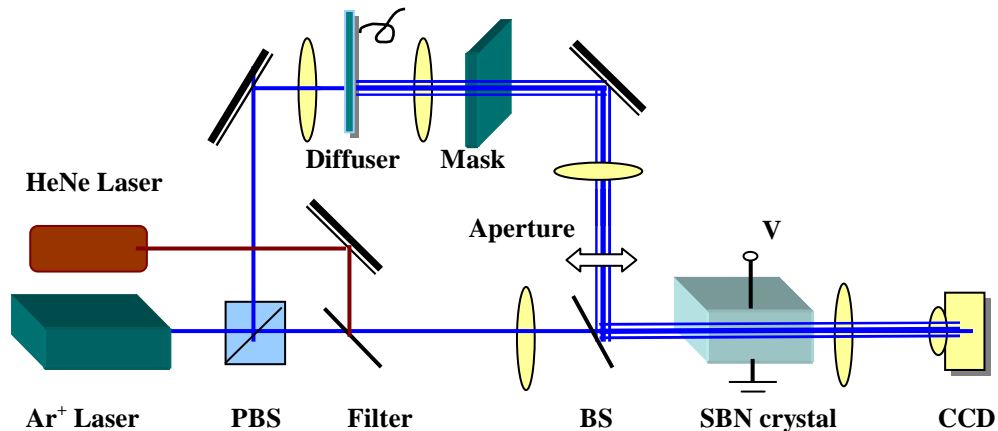


Fig. 1. Experimental setup. PBS: polarizing beam splitter; SBN: Strontium Barium Niobate.

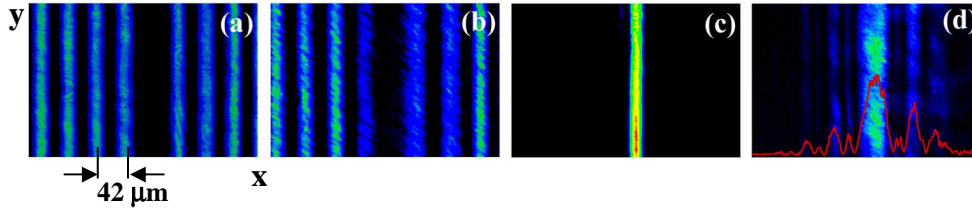


Fig. 2. Transverse intensity patterns of the lattice beam at crystal input (a) and output (b) with a single-site defect, and those of probe beam at input (c) and output (d) after 20-mm of propagation through the defect channel. (Bias field: 1.1 kV/cm).

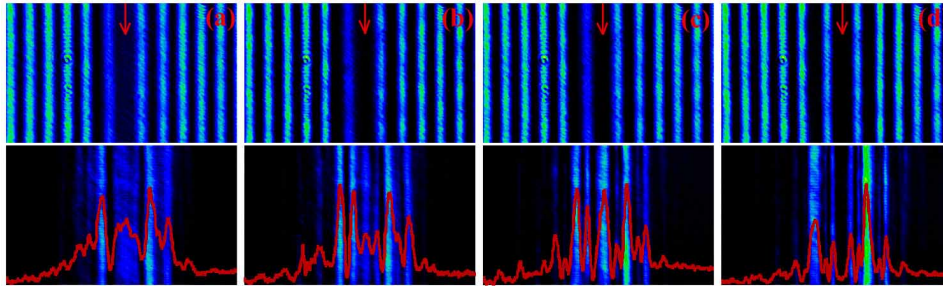


Fig. 3. Top: output lattice pattern with defect site marked by red arrow. Bottom: output probe beam. (a) and (c) correspond to DM in first and second bandgap, respectively. From left to right: bias field is 0.7, 1.1, 1.5, and 2.3 kV/cm for normalized lattice intensity of 0.28. (Lattice spacing is the same as in Fig. 2, but more lattice sites are shown in this figure.)

Typical results are shown in Fig. 3(a-d) for gradual increase of the bias field while other experimental conditions are kept unchanged. The top panel shows the output intensity patterns of the lattice with a negative defect, where the red arrows mark the locations of the defect which was maintained for a large range of the bias field. The bottom panel shows the patterns of the probe beam (initially a Gaussian-like profile launched at the defect site) after 20-mm of propagation collinearly with the lattice beam. From these figures, one can see that the probe beam evolves into a nontrivial intensity pattern after exiting the crystal, but it shows a certain degree of guidance inside the defect in some bias conditions [Fig. 3(a-c)]. Corresponding to the two waveguides next to the defect site, the probe beam either has single peaks [Fig. 3(a)] or double peaks [Fig. 3(c)], suggesting the probe beam evolves into DMs lying in different bandgaps. Under some other conditions, within the defect channel the probe has minimum intensity [Fig. 3(d)], which does not correspond to a DM state. If the bias field is decreased, reversed transition can be realized.

Our theoretical model for a probe beam propagating in the lattice with a defect is [9, 13]

$$iU_z + U_{xx} - \frac{E_0}{1 + I_0 \cos^2 x (1 - f_D(x))} U = 0, \text{ where } U \text{ is the amplitude of the electric}$$

field, z is the direction of propagation, x is the transverse coordinate, I_0 is the lattice peak intensity, E_0 is the applied dc field, and $f_D(x) = \exp(-x^8/128)$ accounts for a local defect. Here all quantities have been non-dimensionalized [13]. In respect to experimental

conditions, one z unit corresponds to about 8 mm, and one E_0 unit corresponds to about 7 V/mm. DMs are found to bifurcate from the edges of different Bloch bands. Typical results for $I_0=0.5$ (close to the experimental value) are displayed in Fig. 4(a-d), where Fig. 4(a) shows the band diagram. The amplitude profiles of DMs show that, in the first bandgap (between the first and second Bloch bands), a DM has one intensity peak with respect to one lattice site [Fig. 4(b)], while a DM in the second bandgap has two intensity peaks with respect to every lattice site [Fig. 4(c, d)]. When E_0 is increased, the DM disappears in lower bandgaps but appears in upper bandgaps. Similar results have been found before [14], but here we used parameters from the experimental conditions, and the bandgaps are narrower than those in [14] due to lower values of I_0 used. The existence or non-existence of DMs and their symmetry behavior has a profound effect on the propagation dynamics of a probe beam aimed into the defect. To illustrate this, we launch a Gaussian beam (16 μm) into the center of the defect at three different bias fields ($E_0 = 4, 11$ and 19). Evolution up to 40 mm is displayed in Fig. 4(e, f, g). At $E_0 = 4$, only one symmetric DM exists in the first bandgap. Correspondingly, the Gaussian beam evolves into that symmetric DM profile upon propagation [Fig. 4(e)]. At $E_0 = 11$, even though there exists a DM in the second bandgap, it is anti-symmetric [Fig. 4(c)], thus the Gaussian beam cannot evolve into that DM but rather diffracts away [Fig. 4(f)]. At $E_0 = 19$, a symmetric DM exists in the second bandgap [Fig. 4(d)]. Consequently, the input beam evolves into this higher-order DM [Fig. 4(g)], whose tails exhibit double peaks in the intensity profile different from that of Fig. 4(e). These characteristics of beam evolution agree well with the experimental results.

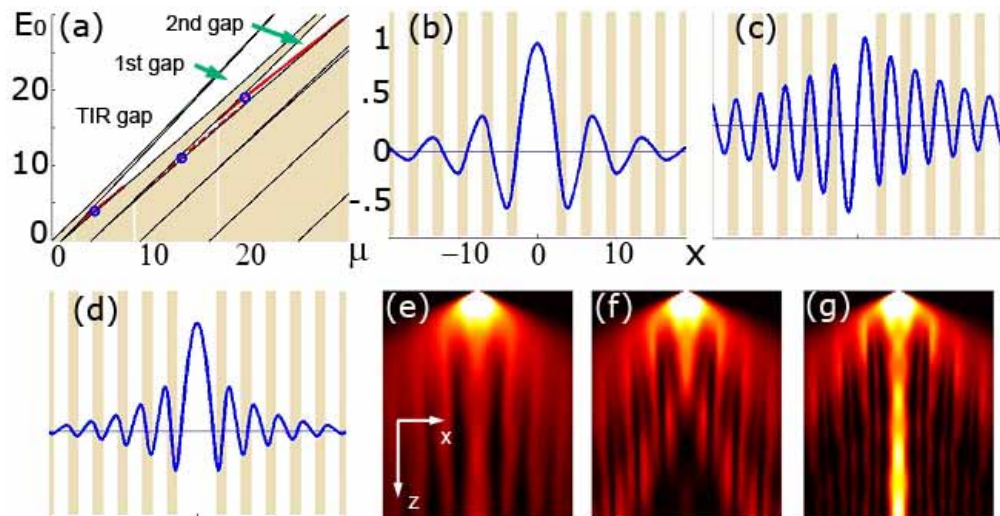


Fig. 4. (a) Bandgap diagram. (b-d) Defect mode solutions at $I_0 = 0.5$ for $E_0 = 4, 11$ and 19, also marked by circles in (a). Shaded stripes correspond to lattice sites. (e-g) Numerical simulations of the evolution of a Gaussian beam through defect for $E_0 = 4, 11$ and 19. Propagation distance: $z=40$ mm. TIR gap indicates the total internal reflection gap or semi-infinite gap.

To further confirm that what we observed indeed corresponds to the DM formation at different bandgaps found in theory, we repeated the experiments of Fig. 3 under slightly

different conditions. Furthermore, we recorded the interferograms between the output probe beam and a broad plane wave to see the relative phase relation of the DM peaks. These results are shown in Fig. 5. At a low bias field (0.5 kV/cm), the output probe beam [Fig. 5(a)] exhibits properties of a DM located in the first bandgap. First, the probe beam maintains a central lobe at the defect site. Second, there is only one intensity peak with respect to each lattice site away from the defect. Third, there is an anti-phase relation between the central lobe in the defect and two side lobes in the tail, since the interference fringes interleave at off-site locations. At a higher bias field of 1.1 kV/cm, the probe beam scatters away from the defect site, indicating the Gaussian beam cannot evolve into a DM under this condition [Fig. 5(b)]. However, as the bias field is increased to 1.7 kV/cm, the beam evolves into a DM of a higher bandgap [Fig. 5(c)]. This can be examined not only from the intensity pattern which shows double peaks corresponding to each lattice site except for the central defect site [see also Fig. 3(c)], but also from the interferogram which shows the anti-phase relation for adjacent peaks. At an even higher bias (2.3 kV/cm), the probe beam scatters away from the defect site again [Fig. 5(d)]. These results illustrate clearly a DM transition from the first bandgap [Fig. 5(a)] to the second bandgap [Fig. 5(c)] as we increase the bias field. These observed DMs are symmetric modes (even functions of x). According to the theory, anti-symmetric modes should also exist under appropriate conditions, for which two peaks with an anti-phase relation within the defect channel are expected [Fig. 4(c)]. However, probing with a symmetric Gaussian profile, we did not observe formation of such an anti-symmetric DM. This suggests that an initially symmetric profile cannot evolve into an anti-symmetric DM, as found also in our numerical simulations.

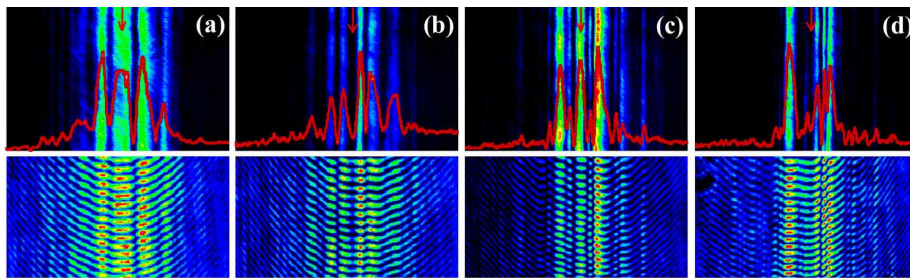


Fig. 5. Top: output probe beam. Bottom: interferogram of the probe beam with a plane wave. From left to right: bias field is 0.5, 1.1, 1.7, and 2.3 kV/cm for normalized lattice intensity of 0.25.

In summary, we have demonstrated for the first time the formation of DMs at different bandgaps of an optically-induced 1D photonic lattice with a negative defect. Guiding light by defect has been demonstrated recently in PCF-like structures with a low-index core as well as in 2D square lattices with a negative defect [20, 21], but in this work we showed controlled excitation of DMs at different bandgaps by tuning parameters. These results have a direct link to earlier pioneering work of using Bragg reflection to obtain lossless confined propagation in waveguide slabs with a dielectric constant lower than the surrounding media [22, 23]. Our results may pave the way for studying many interesting phenomena mediated by defects and defect dynamics in optical lattice structures [24-26].

Acknowledgments

This work was supported by NSF, AFOSR, PRF, NASA EPSCoR, and NSFC. We thank M. J. Ablowitz, D. Neshev, H. Cao, S. Fan and I. Makasyuk for discussion.